Role of Macromolecular Depletion in Red Blood Cell Adhesion

Zhengwen W. Zhang and Björn Neu*
Division of Bioengineering, School of Chemical and Biomedical Engineering, Nanyang Technological University, Singapore

ABSTRACT The adhesion of red blood cells (RBCs) to cells or surfaces is of current basic science and clinical interest yet the details governing this process are still being explored. In this study, the effects of nonadsorbing polymers on the adhesion of RBC to albumin-coated glass have been investigated employing interference reflection microscopy. Our experimental results indicate that adhesion can be induced in the presence of dextran with a molecular mass $\geq$70 kDa and that the induced forces are strong enough to significantly suppress membrane undulations. The overall dependence of the adhesion energies on the polymer concentration is consistent with the assumption that macromolecular depletion induces this attractive interaction. In conclusion, our results indicate that depletion interaction might play a significant role in RBC adhesion via initiating close contacts, and thus suggest the importance of depletion forces for RBC interactions and its relevance to a wide variety of in vitro and in vivo cell-cell and cell-surface interactions.

INTRODUCTION

Cell-cell interactions are governed by interplay of various cell-receptor-mediated interactions and nonspecific forces. Nonspecific forces usually include attractive van der Waals forces, repulsive electrostatic forces, and repulsive undulation forces. If the distance between adjacent cells or surfaces becomes smaller, steric repulsion between surface features will also build up and eventually specific binding between receptor molecules can occur. Thus, understanding how repulsive and attractive nonspecific forces allow or prevent cells approaching one another is a crucial step in order to get a detailed understanding on how cell-cell interaction are controlled in vivo and in vitro.

The adhesion of red blood cells (RBCs) to other cells and to surfaces has been of interest for several decades, mostly due to the fact that abnormal adhesiveness to other RBC and to endothelial cells have been linked to the pathophysiology of various diseases associated with vascular disorders (e.g., sickle cell anemia, diabetes, hypertension) (1,2). Despite these past efforts, the detailed mechanisms and the impact of such changes on the pathology of such diseases remains unknown.

Even though prior studies have described several aspects of RBC adhesion in normal and pathologic states, only very few have considered macromolecular depletion as a mechanism inducing cell-surface adhesion (3). A depletion layer develops near a surface in contact with a polymer solution if the loss of configurational entropy of the polymer is not balanced by adsorption energy (4). Within this layer, the polymer concentration is lower than in the bulk phase. If a particle or cell approaches another particle in a solution containing a depleted polymer, then the difference of solvent chemical potential between the polymer-poor depletion zone and the bulk phase results in solvent displacement into the bulk phase and hence, depletion interaction (5). Due to this interaction, an attractive force develops that tends to minimize the polymer-reduced space between particles and cells, thus resulting in flocculation or aggregation.

The existence of depletion layers at the RBC surface has been confirmed in a few studies (6–11), and that depletion is likely to be the driving force in polymer-induced RBC aggregation (12). Such findings are of great importance in that reversible RBC aggregation is known to be a major determinant of the in vivo blood flow dynamics and resistance (13). However, depletion as a possible mechanism initiating close contact of RBCs to other cells or surfaces has hardly been mentioned.

In this work, we studied the adhesion of RBCs by quantitative reflection interference contrast microscopy (IRM) to understand the physical basis for cell adhesion in solutions containing depleted macromolecules, and thus, the possible role of depletion interaction in cell adhesion. IRM is a powerful tool allowing visual examination of cell/surface contact and separation in real time (14,15). It enables dynamic analysis of surface topologies and local membrane-substrate distances of adherent cells to measure adhesion energies (16). This study was designed to quantify cell adhesion to a rigid protein-coated surface in the presence of polymers. Cell adhesion dynamics, membrane undulations, and adhesion energies were quantified as a function of polymer molecular mass and concentration.

MATERIALS AND METHODS

RBC preparation

Blood was obtained by fingerstick using a sterile lancet and used within 4 h. RBCs were separated from whole blood by centrifugation at 1000 *g* for 5 min, and washed three times in isotonic phosphate-buffered saline solution (PBS, 10 mM including 0.2% bovine serum albumin). RBCs were then resuspended at 0.1% hematocrit in either PBS or dextran-PBS solutions:

Submitted April 22, 2009, and accepted for publication June 2, 2009.

*Correspondence: neu@ntu.edu.sg

Editor: Denis Wirtz.

0006-3495/09/08/1031/7 $2.00

doi: 10.1016/j.bpj.2009.06.006

dextran 40 kDa, dextran 70 kDa, or dextran 500 kDa (Sigma Aldrich, Singapore) were dissolved in PBS at the desired final concentrations.

Interference reflection microscopy (IRM)

A model No. IX71 inverted microscope (Olympus, Melville, NY) was modified for IRM. The microscope is equipped with a 100W high-pressure mercury lamp for illumination and a Neofluor 63 ×/1.25 antiflex oil immersion objective (Zeiss, Oberkochen, Germany). A band-pass filter ($dv = 5$ nm, 85%, Omega Optical, Brattleboro, VT) is used to select the green 546.1 nm Hg line. The contrast is enhanced by placing two polarizers in the illumination and observation path suppressing any stray light (17). The interference images were recorded via a charge-coupled device camera (Olympus).

Coverslip preparation

Round glass coverslips (25-mm diameter), were acid-washed and coated with 3-aminopropyl-triethoxy-silane (APES, Sigma Aldrich) as described elsewhere (18). Briefly, the coverslips were soaked in concentrated nitric acid overnight, washed thoroughly with double-distilled water, dried at 50°C for 24 h, and washed twice in anhydrous acetone. The coverslips were then soaked in a 4% solution of APES in anhydrous acetone for 4 min, rinsed with acetone followed by water, and then dried at 50°C. These aminated (i.e., APES-coated) coverslips were stored in a dust-free environment until use.

Experimental protocol

To coat the aminated coverslips with protein, 2% bovine serum albumin (w/v) was incubated with the coverslips for 2 h at room temperature, thereafter gently rinsed with PBS. The coverslips were than fitted into a chamber and mounted on the microscope stage. The chamber was filled with a 0.1% hematocrit RBC suspension using either dextran-free PBS or dextran-PBS solutions as described above. Unless otherwise stated, the RBCs were allowed to settle to the bottom of the chamber for time periods of 3 min before taking IRM images.

Reconstruction of height profiles

The principle of IRM is based on the interference of light reflected at the glass/medium, I_1, and the medium/cell, I_2, interfaces as illustrated in Fig. 1. The intensity profile of the interference pattern as a function of the vertical membrane-substrate distance $h(x)$ can be approximated as (19)

$$I(x) = I_1 + I_2 + 2\sqrt{I_1 I_2}\cos(2kh(x) - \delta_1 + \delta_2), \quad (1)$$

with $\kappa = 2\pi n/\lambda$ denoting the wave vector of the illumination light in the buffer, n being the refractive index of the buffer, and λ being the wavelength.

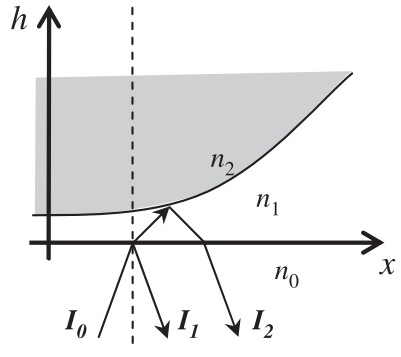

FIGURE 1 Schematic diagram illustrating the image formation by interference of light reflected at the various interfaces; n_0, n_1, and n_2 are the indices of refraction of glass, bulk solution, and cell membrane, respectively.

Since the index of refraction is lower in the medium compared to the RBC membrane, light reflected at the buffer-membrane interface experiences a phase shift of $\delta = \pi$. The cell contour can be obtained by an arccosine transformation of the intensity:

$$h(x) = \frac{\lambda}{4\pi n}\left[\arccos\left(\frac{2I(x) - I_{\max} - I_{\min}}{I_{\max} - I_{\min}}\right) + \delta_1 - \delta_2\right]. \quad (2)$$

Here the intensities are expressed in terms of the measurable maximal intensity $I_{\max}$ and minimal intensity $I_{\min}$.

Contour analysis of height profiles

Analyzing the contour of the cell near the substrates allows computing the adhesion energy in that the shape of the adhering cell is determined by equilibrium of the lateral tension within the fluid membrane and of the bending moment at the boundary. The equilibrium of tension can be expressed in terms of a Young-Dupré equation (20),

$$W = \gamma(1 - \cos\alpha), \quad (3)$$

where α is the contact angle, γ is the surface tension, and W is the adhesion energy (Fig. 2). To get the contact line, a model based on two boundary conditions is used to determine the cell contour at the contact area (21),

$$h(x) = \alpha(x - \lambda) + \alpha\lambda e^{-x/\lambda} \quad (4)$$

for $x \geq 0$. As illustrated in Fig. 2, x is the distance from contact line and λ is the capillary length defined by the distance between the contact line and the intersection of the straight line fitted to the contour of the adhering cell ($x \geq \lambda$),

$$\lambda = \sqrt{\frac{\kappa}{\gamma}}. \quad (5)$$

The contact angle as well as the capillary length can then be determined by fitting the reconstructed cell contour to Eq. 4. The local adhesion energy for different positions at the rim of the cell can then be evaluated assuming a bending modulus $\kappa = 1.8 \times 10^{-19}$ J (22).

RESULTS

Time dependence of RBC adhesion

This study employed 3-aminopropyltriethoxy-silane (APES)-treated surfaces subsequently coated with albumin (3). In a first set of studies, we looked at the impact of the suspending

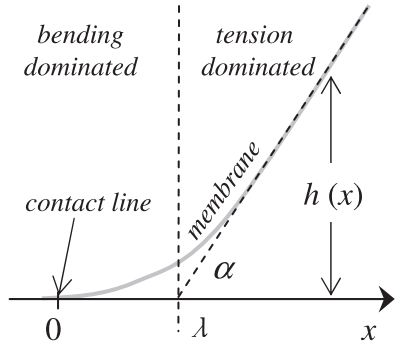

FIGURE 2 Schematic diagram illustrating the height profile with the contact angle α and the capillary length λ of a cell adhering to a flat surface. The onset of the upward deflection ($x = 0$) of the membrane defines the contact line.

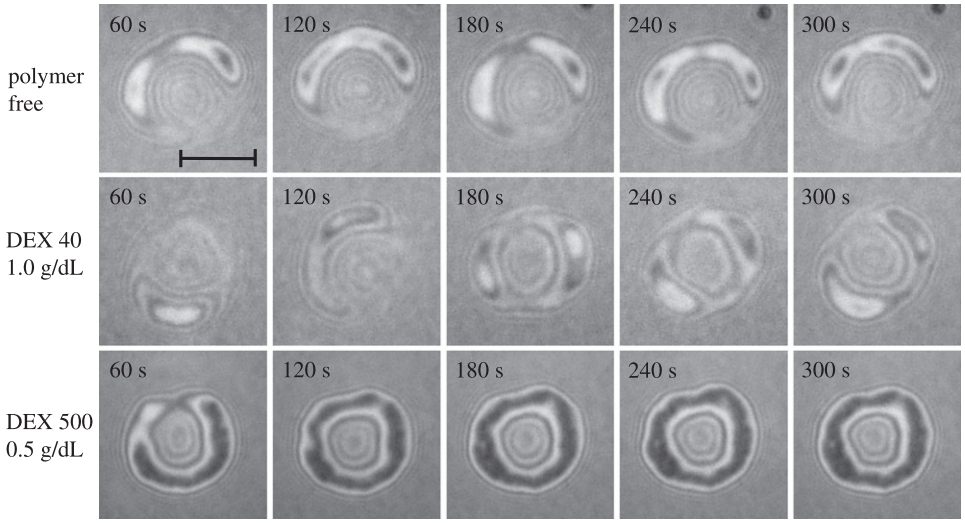

FIGURE 3 Impact of settling time on cell-surface separation in dextran solutions. Time-lapse series of RBC suspended in polymer free PBS (*upper row*), 1 g/dL dextran with 40 kDa (*middle row*) and 0.5 g/dL dextran with 500 kDa (*lower row*). IRM images were taken after different settling times between 60 and 300 s. The scale bar indicates the length of 5 μm.

medium on the dynamics of RBC adhesion to the underlying surface. In Fig. 3, cells suspended in solution containing either no polymer, or dextran 40 kDa (1 g/dL), or dextran 500 kDa (0.5 g/dL), were allowed to settle onto a glass surface, while IRM pictures were taken every 60 s for up to 5 min. In polymer free solution and suspensions containing dextran 40 kDa, the area of close contact stays rather small. Only parts of the peripheral rim of the biconcave RBC seem to be in close contact with the underlying surface. The time dependence of the IRM sequence also demonstrates continuing changes of the cell appearance in polymer free suspension and in dextran 40 kDa solution without significant changes of the overall appearance.

The appearance of the cell suspended in dextran 500 kDa is quite different (Fig. 3, *bottom row*). After 60 s, two-thirds of the cell rim already seems to be in close contact with the underlying surface indicated by the darker appearance of large areas in the IRM picture. After 120 s, the whole outer rim is in close contact, clearly reflecting the donutlike shape of the RBC. This ring of close contact is ~1 μm broad, indicating strong shape changes of the RBC. The overall appearance of the contact area is increasingly noticeable between 60 and 120 s. After 120 s, only small changes can be observed, suggesting significantly tighter binding or closer contact with the underlying surface, as compared to the results obtained in polymer free solution or in the presence of smaller dextran molecules.

Molecular weight dependence of RBC adhesion

To get a quantitative understanding of the cell-surface interface, RBCs were suspended in polymer free suspensions and in solutions containing 1 g/dL of dextran 40 kDa, 70 kDa, and 500 kDa, respectively. The cells were allowed to settle for 3 min and IRM images were recorded. In Fig. 4, images of RBC suspended in polymer free solution (Fig. 4 *A*) and in a solution containing 1 g/dL of dextran 40 kDa (Fig. 4 *B*) are shown as well as light intensities along the lines indicated in the IRM pictures. In both cases, the area of close contact seems rather small, with the settled cells appearing as rings with only small parts of the peripheral rim being in close contact with the underlying surface. In both images, five-to-six dark and bright fringes can be counted between the broad outer rim of the RBC and the center. With a quarter wavelength of 102 nm and the reasonable assumption that the cell surface distance increases monotonically toward the center of the bottom of the cell, this translates to a vertical distance of the bottom of the center and the bottom of the outer rim of ~0.5–0.6 μm. Note that this value is close to the expected stress-free vertical distance of ~0.9 μm (23).

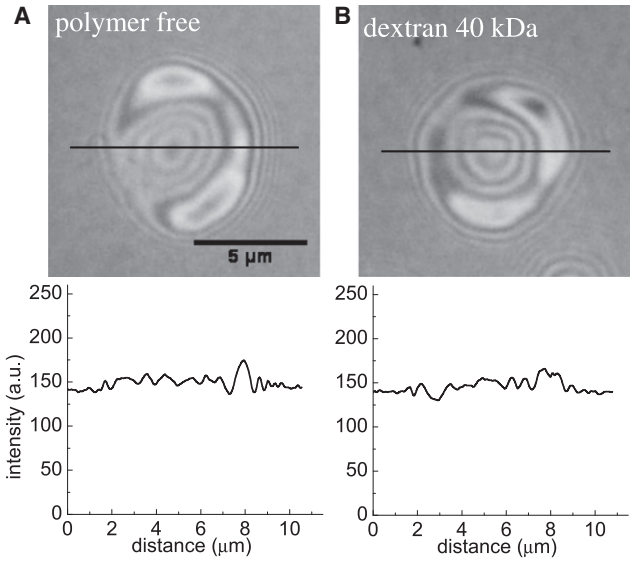

FIGURE 4 Interference reflection microcopy images (*top*) and intensity profiles (*bottom*) along the line indicated in the images of red blood cells adhering to albumin-coated glass surfaces. The cells are suspended in (*A*) polymer free suspension and (*B*) dextran 40 kDa at a concentration of 1 g/dL.

RBCs suspended in 1 g/dL of dextran 70 kDa and 500 kDa seem to be in much closer contact to the underlying surface, as can be seen by the dark appearance of large areas (Fig. 5). In the case of dextran 500 kDa, the whole bottom of the RBC cell seems to be in close contact with the underlying surface due to the presence of this polymer. The presence of dextran 70 kDa at the same concentration only forces the cell rim in close contact with the surface, leaving nine bright and dark circular fringes in the center of the cell. The latter indicates a vertical distance of the center from the rim of ~0.9 μm, again based on the assumption that the distance between the glass slide and RBC increases monotonically toward the center of the cell.

As expected from the intensity profiles and IRM images, large areas are in close contact to the surface with only small spatial fluctuations. Fig. 6 illustrates line-height profiles for RBCs suspended in dextran 70 K solution and 500 kDa, which were reconstructed from the intensity profiles in Fig. 5. The profile of RBC suspended in dextran 70 kDa reveals a flat contact area with a thickness of 0.5–0.6 μm. In dextran 500 kDa, the RBC is in close contact over almost the entire diameter of the cell with the contact area having a diameter at ~7.2 μm.

Membrane undulations in polymer-containing suspensions

As outlined in the previous paragraph, the presence of large dextran molecules induces close contact of RBCs to glass surfaces and the height profiles reveal little spatial fluctuations in the areas of closer contact. In another set of experiments, we studied the vertical membrane undulations as a function of time. In Fig. 7, the absolute membrane undulations of a small patch (~0.015 μm^2) of RBCs either suspended in polymer free solution or in a solution containing dextran 500 kDa at a concentration of 1 g/dL are plotted. The mean value was arbitrarily set to zero. In dextran 500 kDa, these fluctuations stay mostly below ± 5 nm and the standard deviation is 1.7 nm, whereas the undulations in the polymer free suspension are up to ± 10 nm with a standard deviation of 5.2 nm. These results clearly demonstrate that the adhesion forces induced by dextran are strong enough to overcome repulsive membrane undulations.

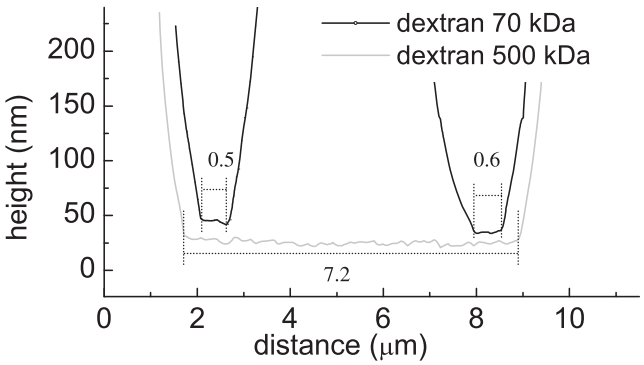

FIGURE 6 Height profile reconstructed from the intensity profiles in Fig. 5.

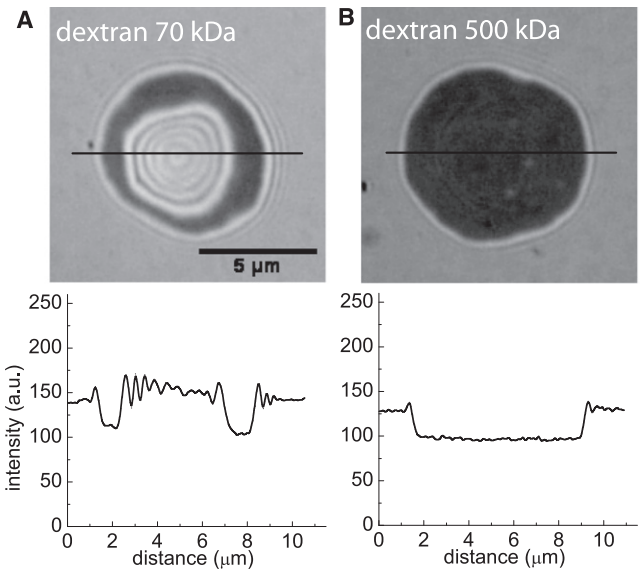

FIGURE 5 Interference reflection microcopy images (*top*) and intensity profiles (*bottom*) along the line indicated in the images of red blood cells adhering to albumin-coated glass surfaces. The cells are suspended in (*A*) dextran 70 kDa and (*B*) dextran 500 kDa at a concentration of 1 g/dL.

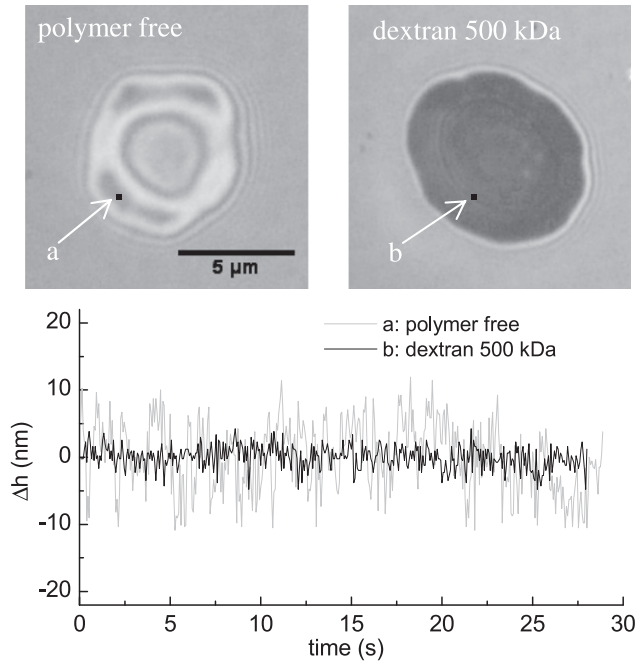

FIGURE 7 Time-lapse of RBC membrane undulations. IRM images (*top*) of RBCs suspended in polymer free solution and in solutions containing 0.5 g/dL dextran 500 K and the undulation amplitude (*bottom diagram*) for a 2 $\times$ 2 pixel area as indicated over a period of 30 s.

Adhesion energies in polymer solutions

By analyzing the contour of the reconstructed height profiles, it is possible to determine the capillary length and the contact angle (Fig. 2) and thus the adhesion energy of RBC in different suspensions. However, due to relative small size of the cells, it is difficult to determine the capillary length at any position along the contact line of the adhering cells (Fig. 8). To overcome this problem, height profiles with clear interference fringes were used to measure the capillary length and thus the membrane tension. The contact angle was than determined for various points by a linear fit to the contour at $x > \lambda$. In Fig. 8, an example is shown of an RBC suspended in a solution containing dextran 70 kDa at a concentration of 0.5 g/dL. The membrane tension was determined to be 52.6 μJ/m^2 leading to adhesion energies between 1.75 and 2.4 μJ/m^2.

To examine the energetics of RBC adhesion by dextran 70 kDa and 500 kDa more closely, the average adhesion energies (Fig. 9 *A*) and contact angles (Fig. 9 *B*) were determined as a function of the polymer concentration. For dextran 70 kDa, a bell-shaped dependence of the adhesion energy and contact angle can be observed (Fig. 9). Starting from the smallest concentration, the adhesion energy steadily increases until it reaches a maximal energy of 8.1 μJ/m^2 at a concentration of 4.0 g/dL. Further increasing the polymer concentration to 8.0 g/dL leads to a dramatic drop of the adhesion energy to 1.5 μJ/m^2. In dextran 500 kDa, the contact angle and adhesion energy also increase monotonically up to a polymer concentration of 4.0 g/dL with a maximal adhesion energy of 13.7 μJ/m^2. Further increasing the concentration leads to a small decline of the adhesion energy and contact angle. The overall dependence seems similar to the one observed in dextran 70 kDa, though the bell-shaped dependence of the energy and contact angles is much less pronounced.

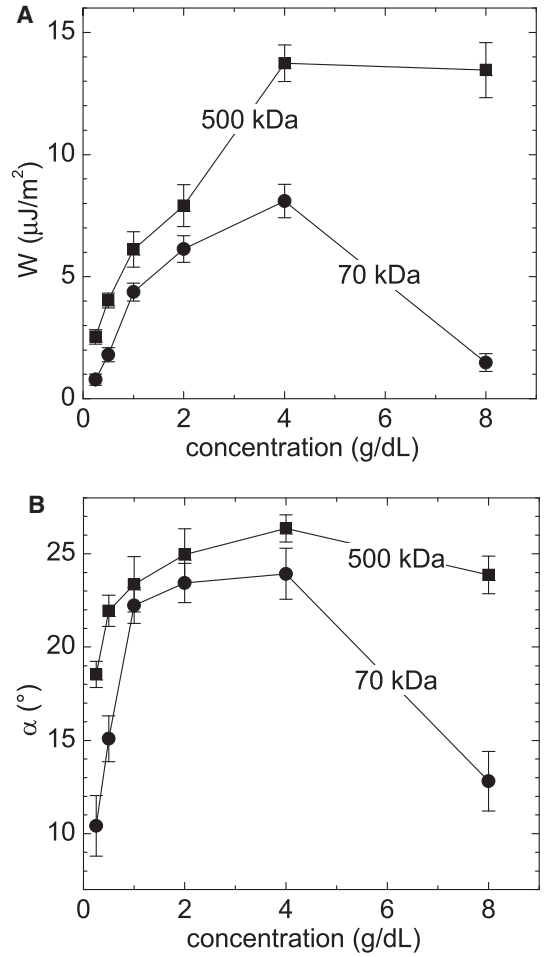

FIGURE 9 Effect of polymer molecular mass and concentration on the adhesion energy for RBCs suspended in solutions of dextran 70 kDa (*circle*) and dextran 500 kDa (*square*). Data points represent averages taken from three cells each.

DISCUSSION

The results clearly illustrate that large dextran molecules can play a significant role in RBC adhesion and that these interactions are strong enough to suppress membrane undulations.

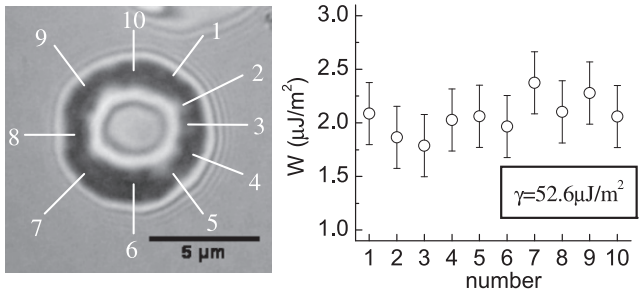

FIGURE 8 Measurement of the membrane tension and the adhesion energy of a red blood cell suspended in 0.5 g/dL of dextran 70 kDa.

Taking into consideration that dextran is a neutral, uncharged polymer without the ability to develop attractive electrostatic interactions and that it has been shown repeatedly that dextran is depleted from the RBC surface (6–11), our findings suggest that these attractive forces are most likely originating from macromolecular depletion. This assumption is also confirmed by the overall dependence of the adhesion energies on the polymer concentration plotted in Fig. 9. For smaller concentrations, a monotonic increase of the energies with the concentration is expected due to the increasing osmotic pressure difference between the depletion zone and the bulk phase. On the other hand, further increasing the polymer concentration will lead to a marked decrease of the depletion layer thickness (24), which will eventually outweigh the increasing osmotic pressure difference (25).

Detailed examination of depletion interaction requires distinguishing between so-called hard and soft surfaces. Hard surfaces are considered to be smooth, not allowing polymer penetration into the surface, whereas soft surfaces, such as

the RBC glycocalyx, are characterized by a layer of attached macromolecules that can be penetrated in part or entirely by the free polymer in solution (4,5). For two adjacent soft surfaces, the depletion interaction energy w_D can be estimated as (25)

$$w_D = -\Pi(2\Delta - d + \delta_1 - p_1 + \delta_2 - p_2), \quad (6)$$

where Π is the osmotic pressure difference, d is the separation distance, Δ the depletion layer thickness, and p and δ represent the penetration depth and thickness of the two adjacent surfaces. Lastly, it is necessary to compute the depletion layer thickness, which can be estimated by (24)

$$\Delta = -\frac{1}{2}\frac{\Pi}{D} + \frac{1}{2}\sqrt{\left(\frac{\Pi}{D}\right)^2 + 4\Delta_0^2}, \quad (7)$$

with the parameter D being a function of the bulk polymer concentration c_b:

$$D = \frac{2k_BT}{\Delta_0^2}\left(\frac{c_b N_a}{M}\right)^{\frac{2}{3}}. \quad (8)$$

Here, k_B and N_a are the Boltzmann constant and Avogadro's number, and Δ_0 is the depletion thickness for vanishing polymer concentration and is equal to $1.4 \times R_g$, where R_g is the polymer's radius of gyration (24).

In Fig. 10, Eq. 6 was employed to evaluate theoretical depletion interaction energies in suspensions containing 40 kDa, 70 kDa, and 500 kDa dextran. Note that in these calculations the thicknesses of the soft surfaces as well as their penetrability were combined with the cell surface separation d to an effective separation $d^* = d - (\delta_1+\delta_2)+(p_1+p_2)$ to reduce the number of variables. Fig. 10 presents calculations with effective separations of 6 nm and 12 nm, respectively. Within the plotted concentration range, all the calculated depletion affinities demonstrate relations that are bell-shaped and concave to the concentration axis. For a larger effective separation of 12 nm, the maximal values of w_d increase with increasing molecular mass. In contrast, a smaller value of d^* yields larger maximal adhesion energies for the smaller dextran of up to ~32 $\mu J/m^2$ in dextran 70 kDa and dextran 40 kDa suspensions, whereas dextran 500 kDa only yields values of up to 15.5 $\mu J/m^2$. Comparing these results with our experimental findings in Fig. 9 shows that the measured values are mirrored by a depletion mechanism, assuming effective separations of ~12 nm for dextran with a molecular mass of 40 kDa or 70 kDa and ~6 nm for dextran 500 kDa. This dependence seems logical, since a larger d^* reflects more penetration of the small polymers into the soft surfaces (26).

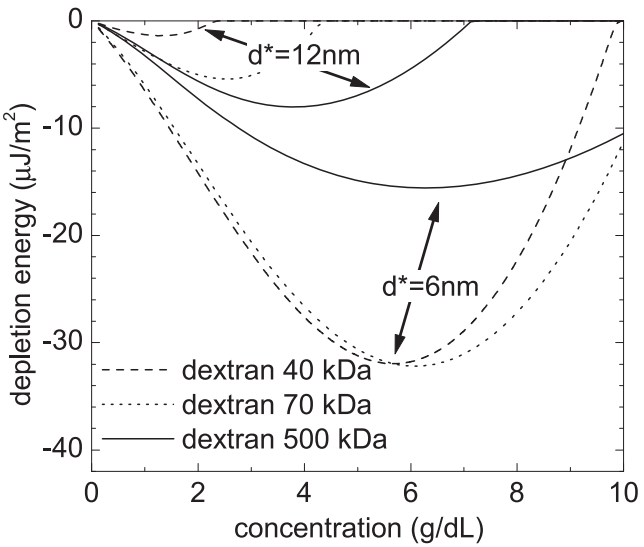

FIGURE 10 Effect of bulk phase polymer concentration c_2 on the depletion interactional energy for two soft surfaces suspended in various molecular mass fractions of dextran with effective cell-surface separations d^* of 6 nm and 12 nm (see text for details).

In conclusion, our results clearly indicate that macromolecular depletion can play a significant role in RBC adhesion and that these interactions are strong enough to suppress membrane undulations. Membrane undulations are a unique feature of soft membranes, and are a consequence of the thermal excitation of bending undulation in the highly flexible bilayer (27). In general, it is believed that undulation forces counteract adhesion and that they are at least partly controlling the in vivo RBC interactions. Thus, even though the experimental system used in this work represents a rather simple in vitro model, our results also suggest that depletion forces could play a significant role for in vivo cell adhesion, in that depletion interaction might promote close cell-cell contacts and thereby allow more-specific adhesive mechanisms to take place.

This work was supported by grants from the Ministry of Education (Singapore) and from A*Star (Singapore, BMRC grant No. 05/1/22/19/382).

REFERENCES

1. Setty, B. N. Y., S. Kulkarni, and M. J. Stuart. 2002. Role of erythrocyte phosphatidylserine in sickle red cell-endothelial adhesion. *Blood*. 99:1564–1571.
2. Wautier, J. L., and M. P. Wautier. 2004. Erythrocytes and platelet adhesion to endothelium are mediated by specialized molecules. *Clin. Hemorheol. Microcirc*. 30:181–184.
3. Neu, B., and H. J. Meiselman. 2006. Depletion interactions in polymer solutions promote red blood cell adhesion to albumin-coated surfaces. *Biochim. Biophys. Acta*. 1760:1772–1779.
4. Fleer, G. J., M. A. Cohen Stuart, J. H. M. H. Scheutjens, T. Cosgrove, and B. Vincent. 1993. Polymers at Interfaces. Chapman & Hall, London.
5. Vincent, B., J. Edwards, S. Emmett, and A. Jones. 1986. Depletion flocculation in dispersions of sterically stabilized particles (“soft spheres”). *Coll. Surf.* 18:261–281.
6. Bäumler, H., B. Neu, R. Mitlohner, R. Georgieva, H. J. Meiselman, et al. 2001. Electrophoretic and aggregation behavior of bovine, horse and human red blood cells in plasma and in polymer solutions. *Biorheology*. 38:39–51.

7. Rad, S., J. Gao, O. K. Baskurt, H. J. Meiselman, and B. Neu. 2009. Depletion of high molecular weight dextran from the red cell surface measured by particle electrophoresis. *Electrophoresis*. 30:450–456.
8. Bäumler, H., and E. Donath. 1987. Does dextran indeed significantly increase the surface potential of human red blood cells? *Studia Biophysica*. 120:113–122.
9. Bäumler, H., E. Donath, A. Krabi, W. Knippel, A. Budde, et al. 1996. Electrophoresis of human red blood cells and platelets. Evidence for depletion of dextran. *Biorheology*. 33:333–351.
10. Donath, E., L. Pratsch, H. Bäumler, A. Voigt, and M. Taeger. 1989. Macromolecule depletion at membranes. *Studia Biophysica*. 130: 117–122.
11. Baskurt, O. K., E. Tugral, B. Neu, and H. J. Meiselman. 2002. Particle electrophoresis as a tool to understand the aggregation behavior of red blood cells. *Electrophoresis*. 23:2103–2109.
12. Neu, B., R. Wenby, and H. J. Meiselman. 2008. Effects of dextran molecular weight on red blood cell aggregation. *Biophys. J*. 95:3059–3065.
13. Baskurt, O. K., M. R. Hardeman, H. J. Meiselman, and M. W. Rampling, editors. 2007. Handbook of Hemorheology and Hemodynamics. IOS Press, Amsterdam, The Netherlands.
14. Gingell, D., and I. Todd. 1979. Interference reflection microscopy. A quantitative theory for image interpretation and its application to cell-substratum separation measurement. *Biophys. J*. 26:507–526.
15. Gingell, D., and I. Todd. 1980. Red-blood-cell adhesion. 2. Interferometric examination of the interaction with hydrocarbon oil and glass. *J. Cell Sci*. 41:135–149.
16. Albersdörfer, A., T. Feder, and E. Sackmann. 1997. Adhesion-induced domain formation by interplay of long-range repulsion and short-range attraction force: a model membrane study. *Biophys. J*. 73:245–257.
17. Verschueren, H. 1985. Interference reflection microscopy in cell biology: methodology and applications. *J. Cell Sci*. 75:279–301.
18. Cooke, B. M., S. Usami, I. Perry, and G. B. Nash. 1993. A simplified method for culture of endothelial cells and analysis of adhesion of blood cells under conditions of flow. *Microvasc. Res*. 45:33–45.
19. Rädler, J., and E. Sackmann. 1993. Imaging optical thicknesses and separation distances of phospholipid vesicles at solid surfaces. *J. Phys. II (Fr)*. 3:727–748.
20. Evans, E. A. 1974. Bending resistance and chemically induced moments in membrane bilayers. *Biophys. J*. 14:923–931.
21. Bruinsma, R. 1995. Adhesion and rolling of leukocytes: a physical model. Proceedings of the NATO Advanced Study Institute on Physics and Biomaterials. NATO ASI Series 332.
22. Evans, E. A. 1983. Bending elastic modulus of red blood cell membrane derived from buckling instability in micropipette aspiration tests. *Biophys. J*. 43:27–30.
23. Skalak, R., A. Tozeren, R. P. Zarda, and S. Chien. 1973. Strain energy function of red blood cell membranes. *Biophys. J*. 13:245–264.
24. Vincent, B. 1990. The calculation of depletion layer thickness as a function of bulk polymer concentration. *Coll. Surf*. 50:241–249.
25. Neu, B., and H. J. Meiselman. 2002. Depletion-mediated red blood cell aggregation in polymer solutions. *Biophys. J*. 83:2482–2490.
26. Neu, B., S. Sowemimo-Coker, and H. Meiselman. 2003. Cell-cell affinity of senescent human erythrocytes. *Biophys. J*. 85:75–84.
27. Helfrich, W. 1978. Steric interaction of fluid membranes in multilayer systems. *Zeitschrift Fur Naturforschung Sect. A-A. J. Phys. Sci*. 33: 305–315.